

Polymer Blending via Near Net-Shape Manufacturing

*Ryan Schexnaydre and Brian S. Mitchell**

Department of Chemical and Biomolecular Engineering

**Tulane Institute for Macromolecular Engineering and Science*

Tulane University

New Orleans, LA 70118

The blending of immiscible polymers via conventional melt or solution processes often creates a final product that is not fully compatibilized, i.e., there exists macroscopic phase separation such that poor adhesion at the interface causes material property degradation. There are inherent problems with these traditional equilibrium methods: heat-induced thermal chain scission that gives rise to a broadened molecular weight distribution and phase separation, toxic organic solvents that are rather difficult to completely remove from the blend, potential undesirable side reactions due to the chemical nature of these processes, and inadequate mixing of rather large phase domains that leads to macroscale heterogeneity and unfavorable interfacial thermodynamics [1]. Chemical compatibilization is typically used to combat poor interfacial adhesion between immiscible polymers, but the kinetic and thermodynamic limitations of such chemical crosslinks cannot prevent phase separation or heat-induced property degradation [2].

The ultimate goal of this research is to compatibilize polymer pairs (e.g., PS/PET) that are conventionally immiscible due to one or more factors. These barriers include large differences between blend components in terms of morphology and crystallinity, glass transition temperature (T_g), particle size and molecular weight. Nonuniform mixing is a detrimental process-related phenomenon that also prevents compatibilization. Finer dispersion resulting from small interfacial tension have large interfacial thicknesses and are more compatible [3]. The interest in compatibilization, therefore, arises because synergistic properties, controlled by the interface, often result when dispersed-phase domain sizes are on the order of a micron or less [2]. Thus, a novel method for blending polymers that addresses the aforementioned technical barriers and can resist macroscopic phase separation upon thermal annealing is suitable for the compatibilization of immiscible polymers.

Near net-shape manufacturing (NNSM) is a solventless, solid-state polymer blending route that can overcome the equilibrium-related phenomena of conventional methods. Figure 1 illustrates the various steps that comprise NNSM. High-energy mechanical alloying (MA) physically forces polymers together through mechanical impact and welding, and this first step of NNSM adds energy to the system through amorphization, particle size reduction, and intimate mixing such that the binary mixture is taken far from equilibrium [4]. Mechanical pressing of these milled powders is followed by isostatic pressing at

room temperatures – a step that fully densifies the blends and eliminates the need for an additional thermal shaping step often found after the blending in traditional schemes. The idea is that the forced physical entanglements during MA can be maintained with increasing temperatures, e.g., those found in a typical melt process, via this pressure-induced retention of interfacial adhesion.

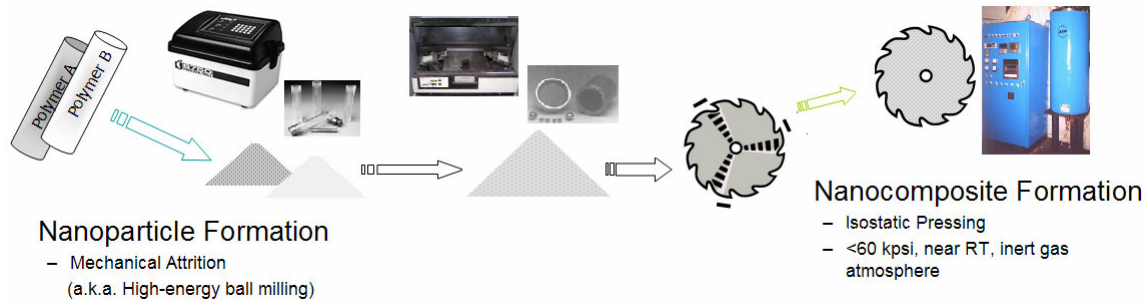


Figure 1: Schematic of Near Net-Shape Manufacturing (NNSM) of binary polymer blends. Appropriate equipment is shown for the two steps of this process.

High-energy ball milling (HEBM) has been studied thoroughly for mechanical alloying of dissimilar metals by Koch [5]. Severe plastic deformation induced by M drives amorphization, particular at lower temperatures. Smith et al. have described the effects of HEBM on molecular weight, crystallinity, and mechanical properties of selected polymers and blends at both cryogenic and ambient temperatures [2]. For example, MM increases the polydispersity index with milling time for both ambient and cryogenic milling of polymethylmethacrylate (PMMA), and cryogenic milling degrades molecular weight more slowly than ambient milling. These molecular weight reductions correspond to analogous decreases in T_g . Font et al. studied crystallization of polyethylene terephthalate (PET) and other polymers, and they found that initially more crystalline polymers amorphized to a greater extent than initially more amorphous polymers (e.g., polyetherimide, PEI) [6]. The rates of these MM-induced decrystallizations were not as sudden as those evidenced in melt or solution quenching, meaning that morphological changes are not as drastic.

In order to ensure that these literature trends were indeed reproducible, experiments were done with some of the polymers shown in Figure 2. The goals of these early investigations were to evaluate particle size reduction, look for contamination, determine if and how much milling affects molecular weight and crystallinity, and verify that the NNSM process is ready for the next step – the alloying of polymers. The polymers used in these and further experiments are mostly readily available commodity polymers with well-known properties. They were also selected such that any random pair (e.g. PS/PET) is very likely to be immiscible. This is crucial because later studies involve attempts to compatibilize these immiscible binary polymer mixtures through NNSM.

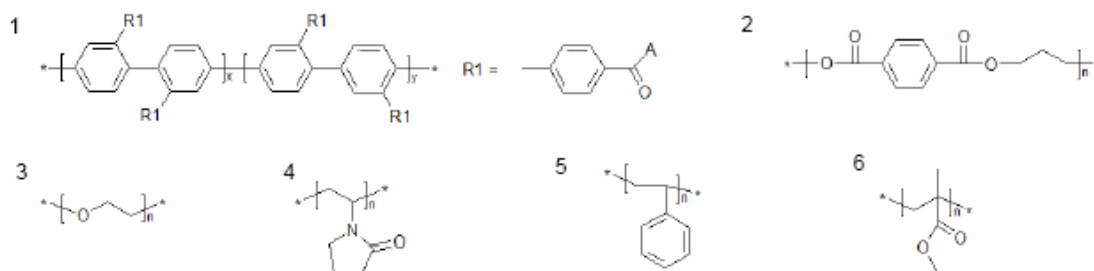


Figure 2: Chemical structures for polymers (1) poly (p-phenylene) PPP, (2) polyethylene terephthalate PET, (3) polyethylene oxide PEO, (4) polyvinylpyrrolidone PVP, (5) polystyrene PS, (6) polymethylmethacrylate PMMA

Preliminary studies were performed to determine if MM produced a substantial amount of ultrafine particles (< 1000 microns). PPP (Figure 2.1), being a high-temperature, hard thermoplastic, was chosen for this analysis. Both ambimilling and cryomilling apparatus in Figure 1 generated ultrafine particles, and cryomilling introduced less contamination to the sample than did ambimilling – not surprising because it had been shown previously that SPEX 8000 mills introduce iron and chromium contamination [7]. As milling time increased, a higher fraction of ultrafines was generated, but agglomeration of the smallest particles ensured that continuous particle size reduction did not occur.

Molecular weight characterization via GPC and light scattering in series was performed to determine if MM affected the molecular weight distribution (MWD) of polymers. PEO and PVP (Figures 2.3 and 2.4, respectively) were selected for these experiments due to their simple structures and water solubility. PEO showed no change in MWD size and shape, while PVP did show negligible broadening of its MWD. This is consistent with the fact that PVP is more likely to undergo scission due to C-N bond presence as well as the fact that PVP has much more amorphous content relative to PEO, leaving more chains exposed at amorphous/crystalline interphase regions.

The amount of crystallinity for PEO and PVP was then calculated via X-ray diffraction (XRD) and differential scanning calorimetry (DSC) with methods outlined in the literature by Chung and Scott [8] and numerical integration. The agreement between the two techniques was pretty close, i.e., differences in percent crystallinities were 5-10% on average. The initially more crystalline (75%) PEO lost more crystallinity than the more amorphous (30%) PVP. This amorphization driving force agrees with the findings of Font et al. [6]. Full width half max (FWHM) data from XRD also showed this change in terms of crystallite size – PVP had a lower crystalline size than PEO initially (1.5 nm vs. 23 nm), and its crystallite size remained relatively unchanged with milling as PEO's decreased as it amorphized. The energy imparted from MM thus changed the two polymers in inherently different ways. PEO had more crystallinity to destroy and few chains in the interphase for scission, while PVP had little crystallinity and more chains exposed for mechanical chain scission.

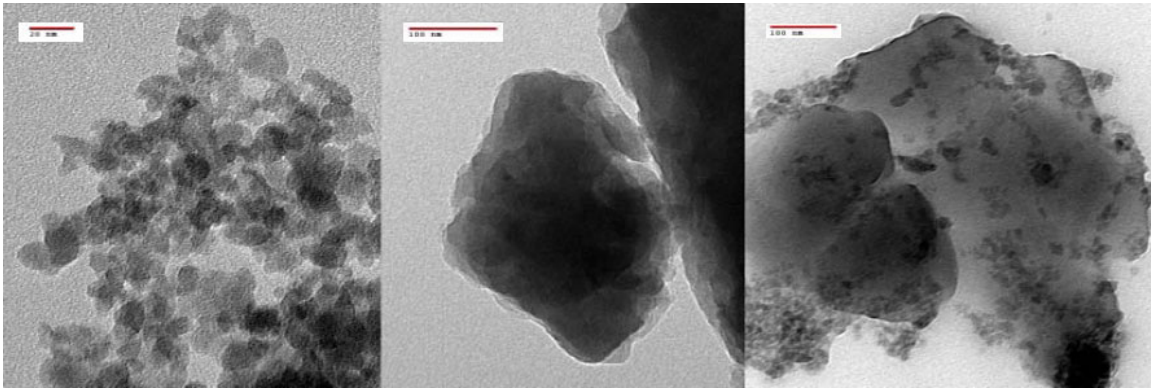


Figure 3: TEM images of PEO (left), PPP (middle), and 50/50 blend of PEO/PPP (right) with bar markers of 20, 100, and 100 nm, respectively. Crystallite size of PEO seen here with TEM compares well with XRD results.

Microscopic techniques were first used to characterize polymer blends processed via NNSM. Transmission electron microscopy (TEM) images shown in Figure 3 reveal very interesting facts. First, the crystalline domains of PEO seen in the left image are approximately the same average size as those measured by XRD, meaning that the data are consistent. Secondly, these PEO domains contrast well with the more amorphous, darker PPP particles in the right image. The immiscible polymers are sticking to each other, showing that milling forces these two polymers together. Scanning electron microscopy (SEM) was also used to study blends made by NNSM, but issues such as sample charging and poor contrast between polymers make it relatively more difficult to utilize. Although microscopic methods have excellent resolution, contrast between polymers often requires further steps, e.g., selective leaching or staining of a blend component.

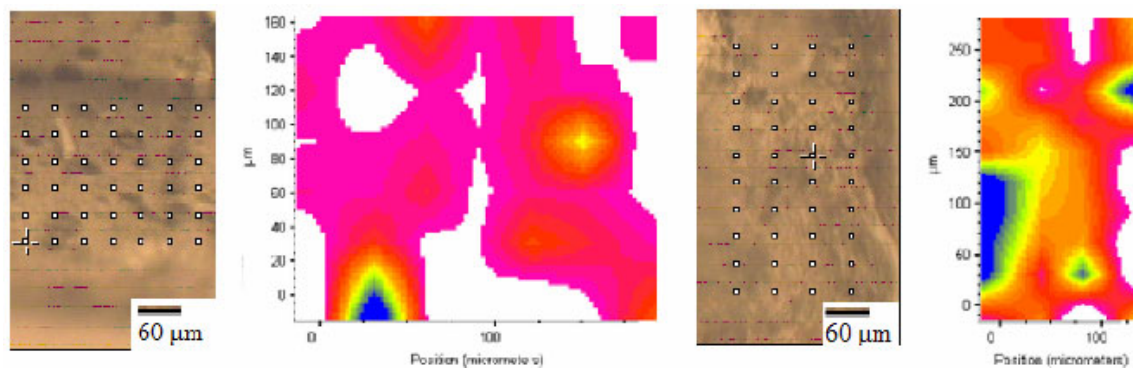


Figure 4: Optical photographs and peak intensity contour area maps for nominal 50/50 (by wt.) blends of PS/PET and PET/PMMA (left and right, respectively). Dispersed phases for these blends are PS and PET, and peaks used for map creation are 3061 and 1508 cm^{-1} , respectively.

Spectroscopic methods were then used to identify milling-induced changes in polymers and their blends. Fourier transform infrared spectroscopy (FT-IR) was predominantly performed because of its relative ease of operation and availability. Initial tests were done with globar FT-IR to look for changes in spectra with milling and the convolution of component spectra into the blend spectrum. However, it had been shown in the literature that FT-IR microspectroscopy with synchrotron radiation can chemically map thin sections of melt-blended polymers with high throughput and low signal-to-noise ratios as well as illustrate concentration gradients of solution-cast blends [sources]. Thus, blends consisting of PS, PET, and PMMA (Figure 2.2, 2.5, 2.6, respectively) were processed with NNSM and then microtomed into thin slices of 5 microns. Figure 4 consists of both the optical photographs taken from the microscope and the corresponding 2-D chemical area maps for two such blends. The maps were created by choosing one of the polymer blend components, typically the dispersed phase, and selecting an absorption peak associated with that particular polymer. For instance, the 3160 cm^{-1} PS aromatic C-H ring deformation and the 1508 cm^{-1} PET aromatic C=C para-substituted stretching transition were selected to create the intensity maps (which can then be correlated to concentration).

Polymer(s)	ΔT_g , C	T_c , C	Crystal peak width, C	T_m , C	Melting peak width, C
PET	22.3	128	21.5	261.5	27.5
PS/PET co-milled	16.4	118.7	30.6	254.8	34.7

Table 1: Thermal transitions and peak widths from DSC plots using thermal analysis software for PET and a 50/50 blend of PS/PET. Incorporation of PS with PET reduces the difference in T_g between the polymers, depresses the melting and crystallization points of PET, and broadens those peaks – all indicators of blend compatibility.

DSC is used extensively in the study of polymer blends. Not only can it be used to identify thermal transitions, but it can also be used to both qualitatively and quantitatively show the blending of two polymers. The blending of PS and PET via NNSM is shown in Table 1. The T_g s of pure PET and PS were found to be 76 and 98.3 °C – values that agree well with those found in the literature [9, 10]. Upon blending, the T_g s of the two polymers converge towards each other, implying that there is some mutual dissolution. The PET in the blend crystallizes at a lower temperature than the pure PET and also has a broader crystallization peak – indicative of a slower crystallization rate than pure PET [9]. The melting peak temperature of PET is decreased and its peak width is broadened in the blend. The PET crystal imperfection and size distribution are increased due to the presence of PS. More studies need to be done to quantitatively compare these peak changes to those of melt-blended polymers.

In conclusion, the ultimate goal of this research is to create novel solid-state polymer blends that could not have been compatibilized via conventional processing methods. Thus, current studies involve direct comparisons between NNSM and melt-blended polymers via DSC, synchrotron FT-IR, and optical microscopy. The interface between polymers in these blends controls their morphologies and properties, so simple model studies with TEM are currently being performed. Future studies could involve interfacial energy determination via contact angle experiments. The focal point of the compatibilization in NNSM is the application of very high pressures (~ 45 kpsi) during isostatic pressing. It will be interesting to find out how much the T_g s of the polymers increase with increasing pressure and to possibly relate this increase to the temperature at which the blend macroscopically shows phase separation. A final relationship between initial pre-milling parameters (molecular weight ratio, composition, and crystallinity) and post-NNSM morphologies will also further explain the interfacial phenomena that occur during NNSM.

References

1. Smith, A.P. et al. *Polymer*, **41**, 6271-6273 (2000)
2. Lebovitz, Andrew H. et al. *Macromolecules*; **35**, 8672 (2002)
3. Paul, D.R. and C.B. Bucknall. *Polymer Blends: Formulation*. Vol 1. John Wiley & Sons, Inc. (2000)
4. De Castro, C. and B.S. Mitchell in: "Nanoparticles from Mechanical Attrition"; Baraton, M.I., Ed.; *Advances in Nanophase Materials and Nanotechnology*; American Scientific Publishers, Los Angeles, CA (2002)
5. Koch, C.C. *Mat. Trans.*; JIM, **36** (2), 85-95 (1995)
6. Font, Joan et al. *Mat. Res. Bul.*; **34**, 2221-2230 (1999)
7. De Castro, C. and B.S. Mitchell. *J. Mat. Res.*; **17** (12), 2997-2999 (2002)
8. Chung, F.H. and R.W. Scott. *J. Appl. Cryst.*; **6**, 225-229 (1973)
9. Ju, M.Y. and F.C. Chang. *Polymer*; **41**, 1723-1726 (2000)
10. Ju, M.Y. and F.C. Chang. *J. Appl. Polym. Sci.*; **73**, 2035-2036 (1999)